

## **Inventory of Supplemental Information**

### **Supplemental Experimental Procedures**

#### **Supplemental Figures and Legends**

Figure S1, related to Figures 1

Figure S2, related to Figure 2

Figure S3, related to Figure 2 and 3

Figure S4, related to Figure 4

Figure S5, related to Figure 5

Figure S6, related to Figure 6

#### **Tables Titles**

#### **Supplemental References**

### **Supplemental Experimental Procedures**

#### **Mice**

B6;129S6-Lrp8<sup>tm1Her/J</sup> (#003524) and B6C3Fe a/a-ReInrl/J (#000235) or wild type mice for neuronal cultures mice were obtained from The Jackson Laboratory.

#### **Contextual fear conditioning**

For contextual fear conditioning experiments we used 11 Reeler WT (6 male, 5 female), 27 Reeler HET (17 male, 10 female), 24 LRP8-WT (12 male, 12 female), and 17 LRP8-KO (9 male, 8 female) mice. The WT and experimental mice were littermates and/or matched for age. The HRM mice were 12-18 wk old at testing and the LRP8-KO mice were 12-16 wk old. Mice were housed under reversed light conditions (8:00AM lights off, 8:00PM lights on) for at least one week to acclimate and then were tested between 9:00 and 11:00AM. Specifically, on the training day, mice were placed in the conditioning chamber for 120 s followed by the onset of a conditioned stimulus (75 dB tone) lasting 30 s. Immediately following the tone offset a 2 s foot shock (0.8 mA, scrambled current) was delivered. The mice remained in this context for another 120 s before a second identical tone-shock pairing was introduced. The mice were returned to their home cages following an additional 150 s in the shock-paired context. 24 hr later, contextual conditioning (as determined by freezing behavior) was measured in a 5-minute test in the chamber where the mice were trained (context test). Freezing behavior (i.e., the absence of all voluntary movements except breathing) was measured in all of the sessions by real-time digital video recordings calibrated to distinguish between subtle movements,

such as whisker twitches, tail flicks, and freezing behavior. Freezing behavior in the context test is indicative of the formation of an association between the environment and the shock; i.e. learning has occurred. Reeler HET mice had significantly lower freezing times than WT mice ( $F(1,34) = 10.8, P = 0.002$ ). There were no significant effects of sex ( $F(1,34) = 3.8, p = 0.06$ ) nor a sex x genotype interaction ( $F(1,34) = 0.92, p = 0.34$ ). Similarly, the LRP8-KO mice froze significantly less than the WT mice ( $F(1,37) = 4.4, p = 0.04$ ). Again, there were no effects of sex ( $F(1,37) = 0.33, p = 0.57$ ) or sex x genotype ( $F(1,37) = 0.07, p = 0.79$ ). These results suggest decreased contextual conditioning in the HRM and LRP8-KO mice.

### **Purification of recombinant Reelin protein**

Full-length mouse Reelin protein was cloned as a FLAG-tagged fusion protein and purified as previously described (Lee et al., 2014). Stable cells lines expressing FLAG-Reelin (HEK293S GnTI) were cultured in presence of 500  $\mu\text{g/ml}$  G418 (Geneticin, Sigma). For protein expression, cells were maintained in medium containing up to 2% fetal bovine serum. Briefly, recombinant protein was affinity purified using the FLAG resin (Sigma) following the manufacturer instructions. Affinity purified proteins were eluted in 150mM NaCl, 10mM Hepes, pH 7.4 and concentrated to approximately 7 $\mu\text{M}$ . Aliquots of the purified proteins were separated by SDS-PAGE to check for purity and integrity. Purified protein was used at a concentration of 10nM in neuronal culture medium for times specified in the figure legends. Vehicle treatment was obtained using the elution buffer as specified above.

### **Luciferase Reporter Assay**

For testing activity of LRN enhancers, we selected 7 regions corresponding to LRN enhancers sequences identified as previously described in the manuscript and 2 negative regions where we did not observe binding of any factor or presence of any RNA transcript. The PCR fragments were cloned into the pGL2-Luc vector containing a minimum Fos promoter by SallI and BamHI. A list of primers used for cloning is provided upon request. pGL2 enhancers reporter constructs were transfected along with Renilla-TK plasmid and 40nM scrambled or LRP8 siRNA (Dharmacon) into DIV3

cortical neurons by using Lipofectamine® LTX with Plus™ Reagent (Life Technologies) following manufacturer's instructions. 24 hours post-transfection, they were subjected to the luciferase assay using the Dual-Luciferase reporter assay kit (Promega); plates were read in Veritas Microplate Luminometer (Turner Biosystems). For Gal4-Luciferase assay, N2A cells were transfected by Lipofectamine 2000 (Life Technologies) following manufacturer's instructions and subjected to same luciferase protocol as described above.

### **qPCR, Data Analysis, and Statistical Analysis**

For qRT-PCR experiments, primary cortical neurons were plated in 48-wells plate and treated for 6 hours before collection. cDNA for qPCR was obtained using Power SYBR Green Cells-to-CT Kit (Life Technologies). Relative quantities of gene expression levels were normalized to GAPDH or 18S. ChIP-DNA samples for qPCR were prepared using the detailed protocol below. The relative quantities of ChIP samples were normalized by individual input DNA samples respectively and fold recruitment values were obtained by comparing each antibody with a control sample (IgG). All qPCRs were performed in MX3000P (Stratagene) using 2X qPCR master mix from Affimetry or Bio-Rad. Results are reported as mean  $\pm$  SD of three independent experiments. Data were analyzed and statistics were performed using unpaired two-tailed Student's t-test. A list of primers used for qPCR is provided (Table S2).

### **Lentivirus Packaging, and Transduction and CRISPR interference experiment**

For cloning gRNAs we used a strategy previously published (Chen et al., 2013; Qi et al., 2013). Briefly, the sgRNAs targeting non-repetitive sequences were designed using a web-based CRISPR design tool (<http://crispr.mit.edu/>). Subsequently, the specific gRNAs were cloned into the same sgRNA lentiviral expression vector by amplifying the insertions using a common reverse primer but unique forward primers containing the protospacer sequence. The PCR fragments were cloned into the vector by BstXI and XhoI. The primer sequences are included in Table S2. The pHR-SFFV-dCas9-BFP-KRAB (#46911), psPAX2 (#12260) and pCMV-VSV-G (#8454) plasmids were obtained from Addgene. Lentivirus package and transduction protocols were conducted as

previously described (Ding and Kilpatrick, 2013). Briefly, lentiviral plasmids were co-transfected with packaging plasmids and into HEK-293-T cells using Lipofectamine 2000 (Life Technologies). Lentiviruses were harvested in NB media 72 hours after transfection and a pool of lentiviruses expressing 4 gRNAs for each enhancer and dCas9-KRAB were used for infection. Neurons were infected at DIV3-4 by incubating neurons for 24 hours with viral particles in NB media. After infection, viral particles were removed and neurons were cultured in original culture media. Treatment and collection was performed 4 days after infection.

### **Total protein extracts and immunoprecipitation**

Primary neurons were collected with cold PBS and lysed with lysis buffer (20mM Tris pH 7.4, 150mM NaCl, 1mM EDTA, 1% IGEPAL, protease inhibitor cocktail). 1mg of total lysate was incubated overnight at 4<sup>0</sup>C with 2ug of antibody pre-bound to 20ul of Dynabeads G. The day after the beads-protein complexes were then washed 3 times with lysis buffer and boiled for Western blots analysis.

### **Nuclear and cytosolic protein extraction**

Cortical tissue samples from WT and mutant LRP8-KO mice were homogenized using a Dounce tissue grinder set in cold 1X HBSS and excessive debris were removed by using a tissue strainer (Pierce) by gentle centrifugation. The cellular pellet was lysed in hypotonic buffer (10mM HEPES pH7.9, 10mM KCl, 1.5mM MgCl<sub>2</sub>, 1mM DTT, 0.2% IGEPAL, protease inhibitor cocktail). Cytosolic fraction was separated from nuclei by centrifugation. Nuclear pellet was washed in hypotonic buffer and lysed in nuclear extraction buffer (20mM Hepes pH7.9, 420mM NaCl, 1.5mM MgCl<sub>2</sub>, 1mM DTT, 25% glycerol, 0.2% NP40, protease inhibitor cocktail).

### **Deep-sequencing**

For all ChIP-seqs, GRO-seqs, RNA-seqs and 4C-seqs, the DNA libraries were sequenced for 50 cycles on Illumina's HiSeq 2000 system according to the manufacturer's instructions. The first 48bp of each sequence tag were aligned to the July 2007 assembly of the mouse genome (NCBI 37, mm9) using Bowtie2 (Langmead and Salzberg, 2012).

Further analysis was performed using only tags that mapped uniquely to the genome. Visualization of the data for ChIP-seq, RNA-seq and GRO-seq was computed by preparing custom tracks on the University of California, Santa Cruz, (UCSC) genome browser using HOMER software package (<http://homer.salk.edu/homer/>). For 4C-seq, the data was visualized using R software package. To facilitate the comparison between different sequencing libraries, the total number of mappable reads was normalized to  $10^7$  for each experiment.

### **Identification of ChIP-seq Peaks, Tag Density Profiles and Scatter plots**

The identification of ChIP-seq enriched regions (peaks) was performed using HOMER similar to our previously published methods (Heinz et al., 2010; Wang et al., 2011). For all experiments, only one tag from each unique genomic position was considered to avoid clonal amplification artifacts from sequencing. Peak finding was determined by identifying significantly enriched clusters of ChIP-seq tags relative to local ChIP-seq signal (>4 tags in 10kb window) and by filtering background signal originated by sequencing of input DNA (>4 more tags than input sample normalized to total count). Regions of maximal density exceeding a threshold with a FDR <0.001 were called as peaks, based on the assumption that randomly distributed tags would naturally form clusters given the large number of tags sequenced. We applied different parameters to identify TFs or histone marks enriched peaks due to distinct patterns of tag distribution. For transcription factor/cofactor binding, read counts were calculated within a 200bp sliding window. In the case of histone marks, initial seed regions of 500bp were considered to calculate enriched reads. Peaks separated by 1kb were merged and considered as blocks of variable lengths. All peaks were then associated with genes by cross-referencing the NCBI Reference Sequence Database (RefSeq). Peaks from individual experiments were considered co-bound by distinct co-factors if peak positions from each experiment located located within 200bp. To generate tag density profiles for all ChIP-seq analysis, tags were counted using 4kb window ( $\pm 2$ kb of the peak center) and 10bp bin size, and plotted using Excel. For GRO-Seq, the tag counts were calculated strand specifically and then plotted as described above. To generate scatter plots, genomic positions corresponding to the overlapping peak positions are defined when the peak centers from individual experiments (MEF2C or MEF2A and CREB) are located

within 200bp of one another. The scatter plots are then created by calculating the log<sub>2</sub> of the normalized tag counts (>40 tags) from two experiments and plotting these values as (x,y) coordinates. For each peak position, the number of normalized ChIP-Seq tags positioned within 200 bp of the center of the peak are counted for each experiment to be compared, for example for CBP. The top 5% CBP peaks were displayed.

### **Motif Analysis**

Motif discovery was performed using a comparative algorithm as described in HOMER (Heinz et al., 2010). Motif finding for TFs was performed on sequence from  $\pm 200$  bp relative to the peak center. Peak sequences were compared to 50,000 randomly selected genomic fragments of the same size matched for CpG% to remove sequence bias introduced by CpG Islands. *De novo* motifs are generally enriched in ChIP-Seq peaks versus the genomic background. Sequence logos were generated using WebLOGO (<http://weblogo.berkeley.edu>).

### **Characterization of LRN Enhancers**

We first identified H3K4me<sub>2</sub>-marked distal enhancers. Then, we defined different enhancers subsets based on the co-occupancy of CBP, CREB, MEF2A and MEF2C. The tag density profiles for promoters are plotted using a 4kbp windows around the TSS of Reelin-regulated genes. The tag density profiles for enhancers are plotted using a 4Kb windows around the center of the enhancers defined as those in which the peak center for each factor (MEF2C or MEF2A, CREB and CBP peak) is within 200bp apart from the others. The tag density profiles include all enhancers identified in a 200kbp window from the TSS of the Reelin-regulated coding genes. eRNA level for each enhancer for computed with strand specificity. Same results were obtained if we defined CBP-occupied enhancers using H3K27Ac mark (data not shown).

### **Radar plot**

The radar plot was computed by calculating the frequency of CREB-bound H3K4me<sub>2</sub>-enhancers and promoters in a window size of 200kb apart from Reelin-regulated coding

genes TSS. The results were compared to three times randomized Reelin-independent genes and P values were calculated using the Fisher exact test.

### **GRO-seq and RNA-seq Analysis**

GRO-seq data analyses were performed as previously reported (Li et al., 2013; Wang et al., 2011). Approximately  $33\text{-}43 \times 10^6$  reads mapping uniquely to the genome were obtained per condition. Briefly, the sequencing alignment step allows maximal 3 unique tags per position. GRO-seq tag density within gene bodies were normalized by the length of the gene, excluding the 400bp promoter-proximal region on the sense strand with respect to the gene orientation by using HOMER. Differentially expressed genes were identified using EdgeR software package (<http://www.bioconductor.org/packages/release/bioc/html/edgeR.html>), and threshold of FDR < 0.001, reads per kilobase per million reads (RPKM) > 0.5, and FC >1.5 was applied. The common artifacts derived from clonal amplification were circumvented by considering maximal three tags from each unique genomic position as determined from the mapping data. For RNA-Seq analysis similar alignment strategy was performed. Read counts were calculated by using HOMER software considering only exonic regions for RefSeq genes. EdgeR software package was then utilized to calculate the significant differentially expressed genes in different treatment conditions using the vehicle or DMSO sample as a common control for each set of experiment. A threshold cutoff of FDR <0.01, reads per kilobase per million reads (RPKM) > 0.5 was applied. Gene ontology analysis was performed using HOMER and results with a cutoff threshold (P-value <10<sup>-5</sup>) were visualized. The genetic association analysis was performed using Web-based DAVID functional-annotation tool (<http://david.abcc.ncifcrf.gov/home.jsp>) and results with a cutoff threshold (P-value <10<sup>-2</sup>) were visualized.

### **4C-seq analysis**

For 4C analysis we applied a bioinformatics pipeline previously described (van de Werken et al., 2012). Contact profiles for the FOS promoter site are visualized based on 2Mbp windows centered on the viewpoint. The data is normalized around the viewpoint. 200kb

window size was used to display near-cis interactions. The bottom subpanel heatmap displays the resolution from 2Kbp to 50Kbp, indicating the length of genome that includes the contact enrichment as unit bin size. The color in the heatmap is used to indicate contact intensity. In the subpanel above, the black curve represents the normalized contact frequency calculated based on the linear-truncated mean values with a resolution of 1kb.

### **Supplementary Figure legends**

#### **Figure S1: Purified full-length Reelin protein activates a transcriptional program co-regulated by NMDA-R signalling, Related to Figure 1**

(A) Coomassie staining of purified Reelin protein separated by SDS-PAGE. Different coomassie bands (#1-4) were excised and sequenced by liquid chromatography tandem mass spectrometry (LCLC-MS/MS) to confirm correct protein sequence (data not shown).

(B) Western blot analysis of purified Reelin protein using anti-FLAG and anti-Reelin antibodies.

(C) qRT-PCRs to validate the activation of selected target coding genes identified by GRO-Seq upon stimulation with Reelin recombinant protein (10nM, 6 h). Data are normalized against *Gapdh*. Data are shown as mean  $\pm$  SD

(D) Pie chart showing genes regulated by bicuculline (50uM, 6 h) assessed by RNA-Seq analysis in cortical neurons (FDR <0.01).

(E) Venn diagram showing the overlap of genes regulated by Reelin and bicuculline in cortical neurons, assessed as described in Figure 1A and S1D.

(F) Scatter plot showing the correlation between Reelin- and Bicuculline-regulated genes. *x* and *y* axis represent log<sub>2</sub> of fold change. Pearson Correlation Coefficient is shown (PCC=0.76)

#### **Figure S2: Additional descriptions of ChIP-Seqs presented used to define LRN enhancers, Related to Figure 2**

(A) Table showing the number of putative distant enhancers elements identified in cortical neurons treated with Reelin recombinant protein (10nM, 1 h) by ChIP-Seqs experiments using active enhancer marks (H3K4me<sub>2</sub>, H3K27Ac, H4K16Ac)



(B) Tag density profiles of ChIP-Seq tag counts of all peaks identified for each transcription factor/cofactor (CBP, MEF2A, MEF2C, CREB, NCoR) before and after Reelin treatment (10nM, 1 h).

(C) Bar histogram showing the level of expression (RPKM) of different isoforms of MEF2 transcription factor family, assessed by GRO-Seq.

(D) Venn diagram showing the genome-wide overlap of ChIP-Seq peaks of MEF2A and MEF2C in cortical neurons after Reelin treatment (10nM, 1 h).

(E) Pie chart depicting the genome-wide distribution of different transcription factors/cofactors on active H3K4me-enhancers in cortical neurons treated with Reelin (10nM, 1 h).

(F) Bar graph showing the CREB binding frequency on distinct regulatory elements. Significant P value is calculated by Fisher exact test (\*\* P<0.0001).

(G) Western blot analysis of co-immunoprecipitation of MEF2C and NCOR complex regulated by Reelin treatment in cortical neurons (10nM, 0.5 h).

(H) Bar graph indicating the number of CBP-marked LRN enhancers showing NCoR recruitment before and after Reelin treatment (10nM, 1 h).

**Figure S3: Active histone marks associated to LRN enhancers, Related to Figure 2 and 3**

(A) Box-and-whisker plots show ChIP-Seq tag counts (log<sub>2</sub>, y axis) for different histone marks in cortical neurons treated with recombinant Reelin protein (10nM, 1 h). The central horizontal bar indicates the median normalized tag distribution. See also Figure 2G.

(B) Western blot results of immunoprecipitation with anti-LRP8 antibody from brain cortex of WT and mutant LRP8-KO mice showing the proteolytical processing of LRP8. See also Figure 3A

**Figure S4: CRISPR-mediated interference by lentiviral infection, Related to Figure 4**

(A) Microscopic images depicting cortical neurons infected with different gdRNAs (Top) Bright-field images of cortical neurons; (bottom) RFP channel detecting gdRNAs.

**Figure S5: Additional 4C-sequencing experiments, Related to Figure 5**

(A) Contact profiles of the *Fos* promoter from cortical neurons (as in Figure 5B).

(B) Contact profiles of the *Fos* promoter from WT hippocampi (as in Figure 5C).

**Figure S6: Learning genes identification, Related to Figure 6**

(A) Pie chart showing the genes regulated during memory formation assessed by RNA-Seq analysis (FDR <0.01) in hippocampi dissected 24 h after training

**Table S1: List of Reelin-regulated genes identified by GRO-Seq, Related to Figure 1**

**Table S2: List of primers used in qPCRs, GRO-seq, 4C-seq, and CRISPR cloning, Related to Experimental procedures**

**Table S3: List of genes regulated during hippocampal-dependent associative learning identified by RNA-seq, Related to Figure 6**

**Supplemental References**

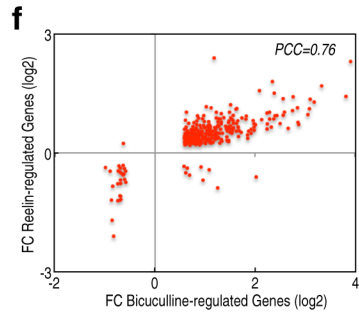
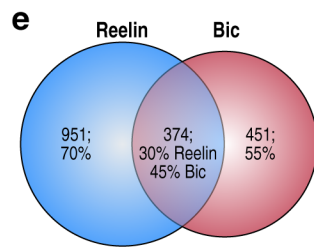
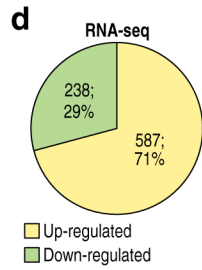
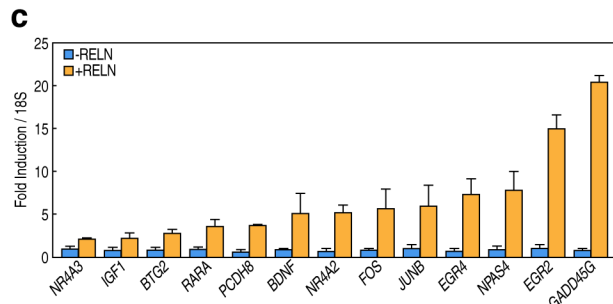
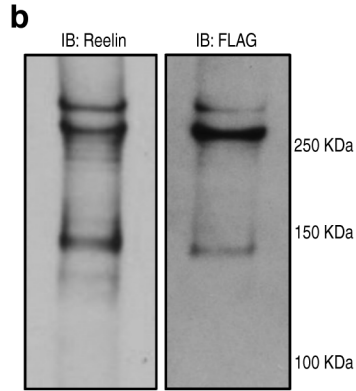
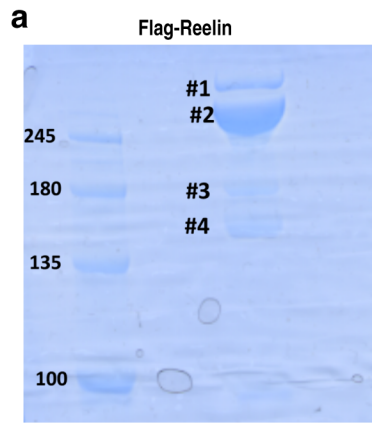
Heinz, S., Benner, C., Spann, N., Bertolino, E., Lin, Y.C., Laslo, P., Cheng, J.X., Murre, C., Singh, H., and Glass, C.K. (2010). Simple combinations of lineage-determining transcription factors prime cis-regulatory elements required for macrophage and B cell identities. *Mol Cell* 38, 576-589.

Lee, G.H., Chhangawala, Z., von Daake, S., Savas, J.N., Yates, J.R., 3rd, Comoletti, D., and D'Arcangelo, G. (2014). Reelin Induces Erk1/2 Signaling In Cortical Neurons Through A Non-Canonical Pathway. *J Biol Chem*.

Li, W., Notani, D., Ma, Q., Tanasa, B., Nunez, E., Chen, A.Y., Merkurjev, D., Zhang, J., Ohgi, K., Song, X., *et al.* (2013). Functional roles of enhancer RNAs for oestrogen-dependent transcriptional activation. *Nature* 498, 516-520.

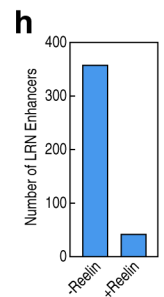
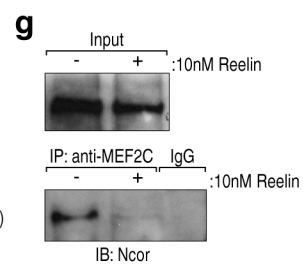
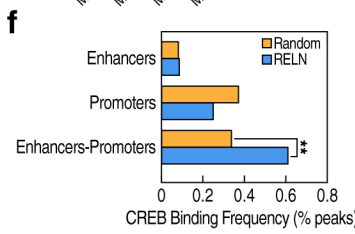
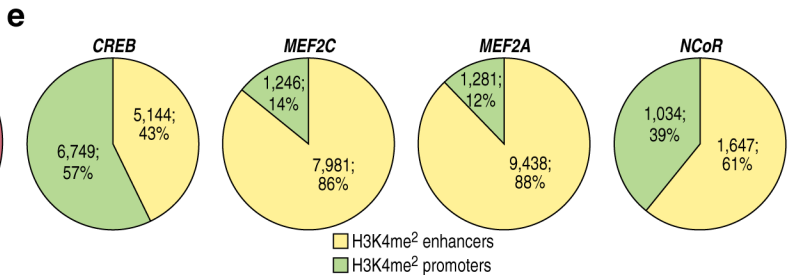
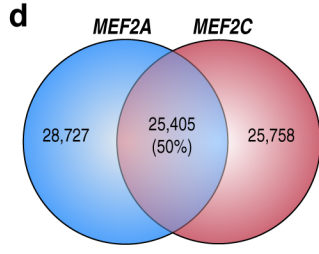
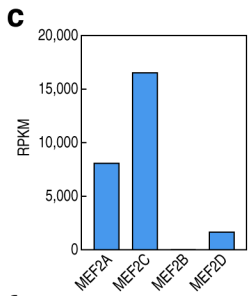
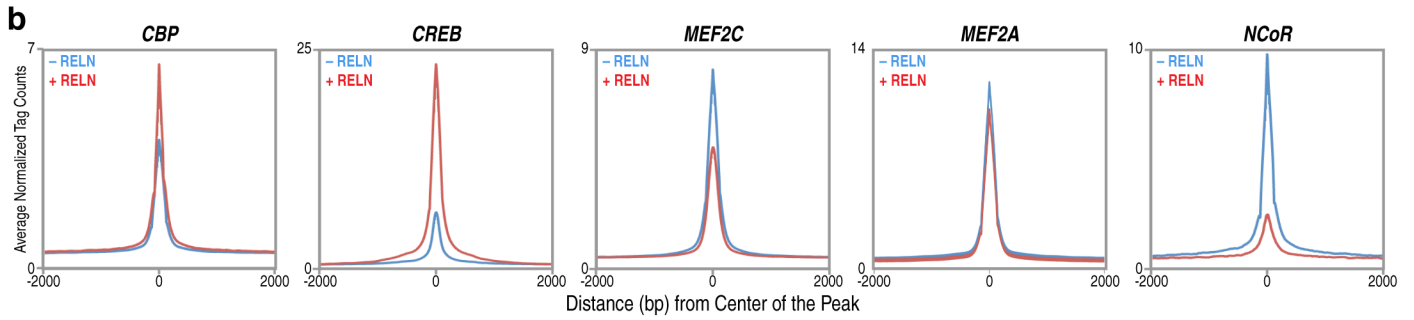
van de Werken, H.J., Landan, G., Holwerda, S.J., Hoichman, M., Klous, P., Chachik, R., Splinter, E., Valdes-Quezada, C., Oz, Y., Bouwman, B.A., *et al.* (2012). Robust 4C-seq data analysis to screen for regulatory DNA interactions. *Nature methods* 9, 969-972.

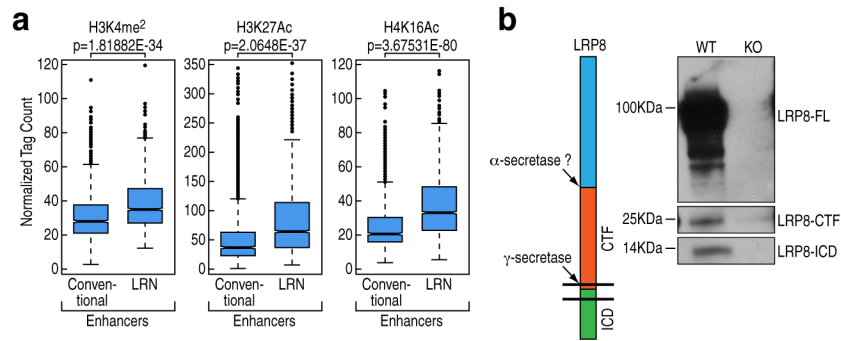
Wang, D., Garcia-Bassets, I., Benner, C., Li, W., Su, X., Zhou, Y., Qiu, J., Liu, W., Kaikkonen, M.U., Ohgi, K.A., *et al.* (2011). Reprogramming transcription by distinct classes of enhancers functionally defined by eRNA. *Nature* 474, 390-394.

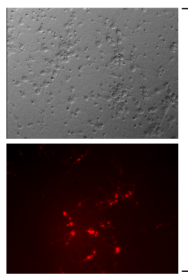


**a**

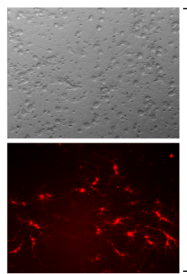
Neuronal enhancers	N. peaks
H3K4me <sup>2</sup>	23,317
H3K27Ac	45,932
H4K16Ac	15,690



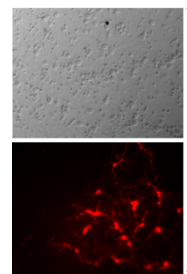




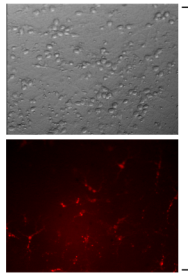
gdRNA-LRNe-*fos3*



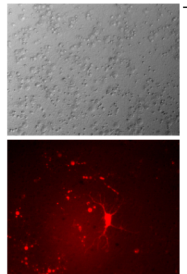
gdRNA-LRNe-*bdnf*



gdRNA-LRNe-*nr4a1*



gdRNA-LRNe-*fos4*



gdRNA-LRNe-*npas4*

